Electronic Supplementary Material (ESI) for Nanoscale.

Supporting information

Au-InSe van der Waals Schottky Junctions with Ultralow Reverse Current and High Photosensitivity

Siqi Hu, Qiao Zhang, Xiaoguang Luo, Xutao Zhang, Tao Wang, Yingchun Cheng, Wanqi Jie, Jianlin Zhao, Ting Mei, Xuetao Gan[*]

Mr. S. Q. Hu, Miss. Q. Zhang, Prof. X. T. Zhang, Prof. J. L. Zhao, Prof. T. Mei, Prof. X. T. Gan

MOE Key Laboratory of Material Physics and Chemistry under Extraordinary Conditions, and Shaanxi Key Laboratory of Optical Information Technology

School of Physical Science and Technology

Northwestern Polytechnical University, Xi'an 710129, China

E-mail: xuetaogan@nwpu.edu.cn (X.G.)

Prof. X. G. Luo, Dr. Y. C. Cheng

Shannxi Institute of Flexible Electronics

Northwestern Polytechnical University, Xi'an 710129, China

Prof. T. Wang, Prof. W. Q. Jie

State Key Laboratory of Solidification Processing

Northwestern Polytechnical University, Xi'an 710072, China

Main Contents

A. Procedures of mechanically stacking electrodes

B. Electrical performances of InSe devices with Au-Au and Ag-Ag electrode configurations

C. AFM characterization of the InSe and *h*-BN flake of the main device

D. Electrical performance of the main device at 77 K

E. Reverse current below 1 pA in Fig. 2(d) extracted from Fig. 2(b)

F. The noise equivalent power (NEP) of the main device

G. The wavelength-dependent photoresponsivity and detectivity of the main device

H. The electrical performance of other devices

A. Procedures of mechanically stacking electrodes

Metal electrodes were first pre-prepared on a smooth silicon substrate. The silicon substrate was cleaned sequentially with acetone, isopropanol, and deionized water to ensure that the surface is sufficiently clean, which was then baked at 400 ºC degrees for half an hour to remove moisture. Patterned Au electrodes were deposited on the silicon substrate by thermal evaporation using a shadow mask. The electrodes were then peeled off from the silicon substrate with PDMS. Finally, the PDMS-bonded electrode was transferred to the InSe sample for electrical contact. The highest transfer temperature (transfer temperature from PDMS to the target substrate) should be kept below 50 ºC to maintain the metal-semiconductor vdW gap and avoid their strong interactions and chemical bond formation.

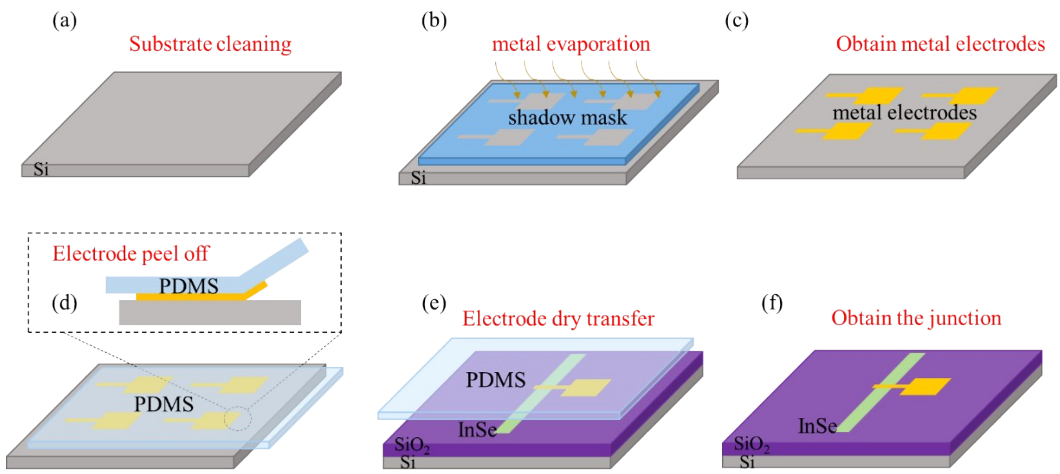

Fig. S1 Technological flow-chart of mechanically stacking electrodes. (a) Cleaning silicon substrate. (b,c) Using metal thermal evaporation and a shadow mask to obtain metal electrodes on the silicon substrate. (d) A piece of PDMS (commercially available, WF-X4-6.0mil, Gel-Pak. Inc) is contacted with the metal electrodes, which are then peeled off by lifting PDMS with sufficiently high speed. (e) The lifted metal electrode is aligned under an optical microscope and physically laminated on an InSe flake. (f) PDMS is removed at a sufficiently low peel speed to allow the electrode to preferentially adhere to the device substrate and separate from the PDMS.

B. Electrical performances of InSe devices with Au-Au and Ag-Ag electrode configurations

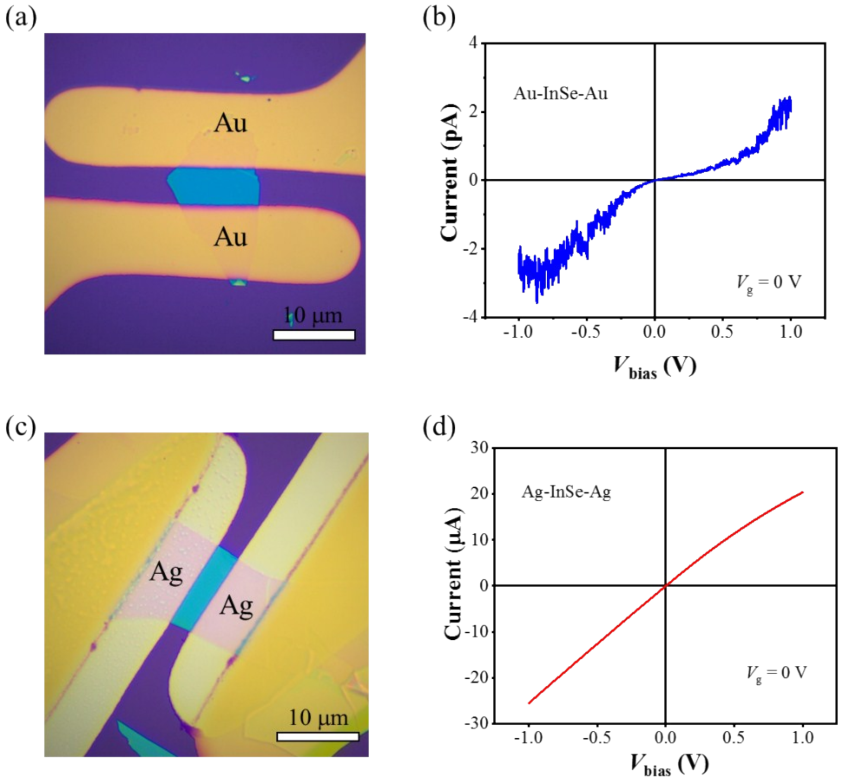

Fig. S2 (a) Optical microscope image of an Au-InSe-Au device. (b) I_{ds}-V_{ds} characteristic of the Au-InSe-Au device. (c) Optical microscope image of an Ag-InSe-Ag device. (d) I_{ds}-V_{ds} characteristic of the Ag-InSe-Ag device.

C. AFM characterization of the InSe and h-BN flake of the main device

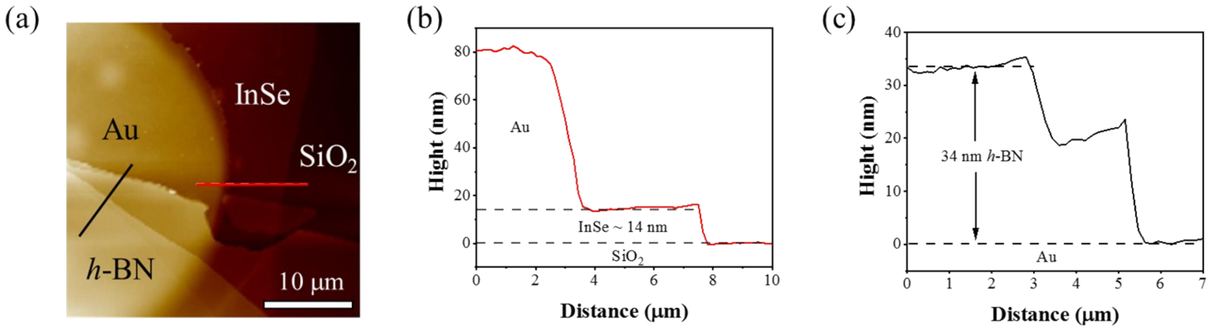

Fig. S3 (a) AFM image of the Au-InSe vdW junction device. (b) Thickness of the InSe flake. (c) Thickness of the *h*-BN flake.

D. Electrical performance of the main device at 77 K

The characteristics of the Au-InSe vdW junction at different V_g were tested at 77 K as well in a home-made liquid nitrogen thermostatic chamber. The test accuracy is approximately 10 pA. The transfer properties were measured with a forward bias (V_{bias} = +2 V) and a reverse bias (V_{bias} = -2 V), as shown in Fig. S4(a). Figure S4(b) shows the gate-dependent output characteristics. Compared with the performance at room temperature, the rectification ratio of the device decreases at 77 K. This result can be attributed to the on/off ratio decrease of the device under forward bias (V_{bias} = +2 V) and the tunneling current increase under reverse bias (V_{bias} = -2 V) at 77 K, as indicated in Fig. S4 (a). And the I_{ds} increases when V_g decreases from -20 to -60 under reverse bias (V_{bias} = -2 V), as shown in Fig. S4 (a), which can be attributed to the emergence of p-type InSe under V_g modulation. This bi-polar behavior of InSe device is out of the scope of this manuscript, which would be discussed elsewhere in our future work.

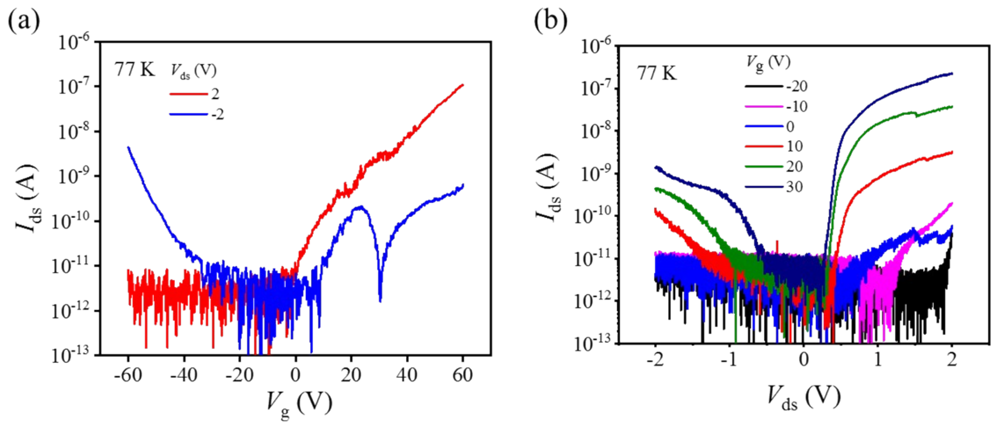

Fig. S4 Electrical characteristics of the Au-InSe vdW Schottky junction device at 77 K. (a) Transfer characteristics of the device with forward (V_{bias} = 2 V) and reverse (V_{bias} = -2 V) bias. (b) Semilogarithmic plots of the output curves at V_g varying from -20 to 30 V.

E. Reverse current below 1 pA in Fig. 2(d) extracted from Fig. 2(b)

Reverse current below 1 pA in Fig. 2(d) is obtained by averaging the reverse current values under reverse bias in Fig. 2(b). As shown in Fig. S5, we draw the four curves in Fig. 2(c) separately, and average the reverse current of each curve as shown in the green line in the pictures.

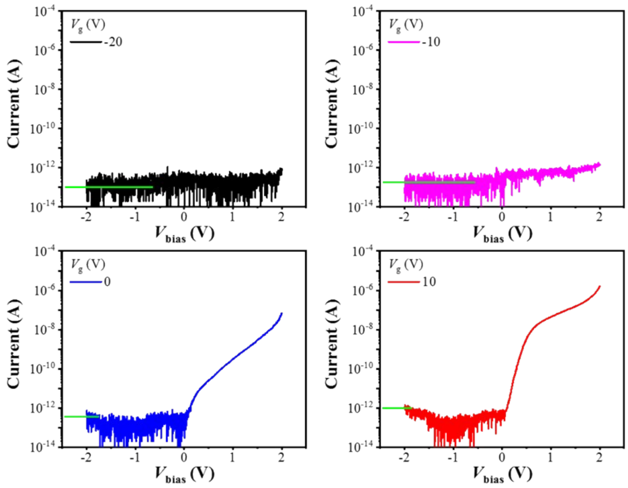

Fig. S5 Semilogarithmic plots of the output curves at V_g varying from -20 to 10 V. The green baselines indicate the average reverse current value under different reverse biases.

F. The noise equivalent power (NEP) of the main device

From the results of the noise current and responsivity under different incident light power, we calculated the NEP as shown in Fig. S6. The NEP is the incident light power at which the signal-to-noise ratio is unity and it is related to the responsivity (R) and the noise current (i_n) by equation:[1] NEP = i_n/R. Since the responsivity R decreases with the increased optical power, the NEP increases with the increased incident optical power.

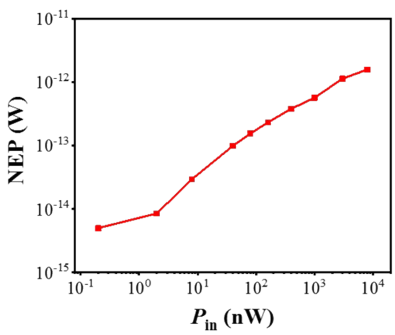

Fig. S6 The estimated NEP of our photodetector with respect to the incident optical power

G. The wavelength-dependent photoresponsivity and detectivity of the main device

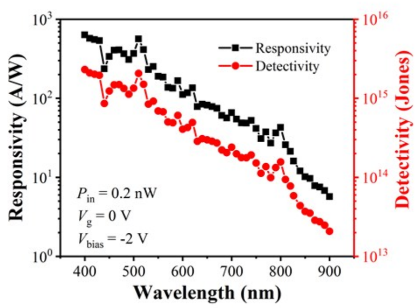

Fig. S7 Photoresponsivity and detectivity of the device for wavelengths ranging from 400 to 900 nm at V_g = 0 V and V_{bias} = -2 V. The laser wavelength was tuned continuously using an acousto-optic turnable filter varying from 400 to 900 nm with an interval of 10 nm.

H. The electrical performance of other Au-InSe-Ag devices

Table S1

	Thickness (nm)	Reverse current (pA)	Rectification Ratio
Device 1	10.3	2	2×10^5
Device 2	11.3	~1	3×10^5
Device 3	13.2	3	2×10^5
Device 4	16.5	<1	1×10^5
Device 5	20.3	~1	1×10^6
Device 6	43.3	~5	2×10^5

From these results, we can see a little variation on the performance from device to device with different InSe thicknesses, which indicates the repeatability of our results.

Reference

[1] Y. Fang, A. Armin, P. Meredith, J. Huang, *Nat. Photon.*, **2018**, 13, 1.